Available online at www.sciencedirect.com
ScienceDirect
Journal of Photochemistry and Photobiology A: Chemistry 197 (2008) 342–350
Journal of Photochemistry and Photobiology A:Chemistry
www.elsevier.com/locate/jphotochem

Photochemistry and photophysics of a morpholino methylthio phenyl ketone: A steady-state, picosecond pump-probe laser spectroscopy and molecular modeling investigation

F. Morlet-Savary *, X. Allonas, C. Dietlin, J.P. Malval, J.P. Fouassier

Département de Photochimie Générale, UMR n°7525, University of haute Alsace, ENSCMu, 3 rue Alfred Werner, 68093 Mulhouse, France

Received 14 November 2007; received in revised form 18 January 2008; accepted 22 January 2008
Available online 6 February 2008

Abstract

The photophysics of 2-methyl-1-[4-(methylthio) phenyl]-2-(4-morpholinyl)-1-propanone TPMK, compared to that of two reference compounds (2-methyl-1-phenyl-2-(4-morpholinyl)-1-propanone and 1-[4-(methylthio)phenyl]-ethanone), was studied by means of absorption spectroscopy, phosphorescence and time-resolved absorption spectroscopy. A four-level kinetic scheme has been proposed for TPMK as an explanation for the observed excited state processes. A strong solvent effect has been noticed upon the excited state lifetimes. Modeling calculations help to describe the excited state properties.

Keywords: Clevage process; Pump-probe spectroscopy; Photoinitiator

1. Introduction

The excited state processes of efficient photoinitiators of radical polymerization have been explored in a lot of studies concerned e.g. with benzoin ethers, hydroxy alkyl phenyl acetophenones, dialkoxy acetophenones, phosphine oxide derivatives, amino ketones, benzophenones, benzils, thioxanthenes ... (see e.g. [1–12]). The effects of the skeletons, substituents, environment as well as the influence of typical modifications to induce enhanced properties have been largely studied through (i) the investigation of what happens in the transient states formed upon light excitation of photoinitiators (PI) and (ii) the evaluation of the photoinitiators performance in polymerization experiments. Few studies, however, have been conducted so far on the three following points: (i) the detection of the very short-lived excited states (present in highly efficient cleavable photoinitiators) [7,11,12] in their own time scale of evolution, (ii) the theoretical analysis of the cleavage reaction (except the earlier works carried out on model ketones [13] or the recent attempts on phosphine oxides [14a]) and cleavable acetophenone derivatives [14b,c] and (iii) the experimental and theoretical investigation concerned with the introduction of suitable substituents on a given structure [14d].

In the present paper, we will select three compounds (Scheme 1) in order to outline the role of a methylthio substitution at the para position of a benzoyl chromophore: (i) 2-methyl-1-[4-(methylthio)phenyl]-2-(4-morpholinyl)-1-propanone TPMK (which is a widely used photoinitiator) and (ii) two reference molecules: 2-methyl-1-phenyl-2-(4-morpholinyl)-1-propanone PMK and 1-[4-(methylthio)phenyl]-ethanone TPK.

Previous estimates provided triplet state lifetimes lower than 1 ns for PMK [1] and in the range of 10 ns for TPMK [15]. These values support a fast Norrish I cleavage taking place from a $n\pi^*$ excited triplet state (Scheme 2 where PI stands for TPMK or PMK). This process yields a (substituted) benzoyl radical and a 2-(4-morpholinyl)-1-propanonyl radical (Scheme 3) which absorb in the UV/near visible wavelength range. TPK should not cleave.

Our study has been conducted through a steady-state investigation, a direct detection of the excited states by pump-probe

* Corresponding author.
E-mail address: fabrice.morlet-savary@uha.fr (F. Morlet-Savary).

1010-6030/$ – see front matter © 2008 Elsevier B.V. All rights reserved.
doi:10.1016/j.jphotochem.2008.01.013

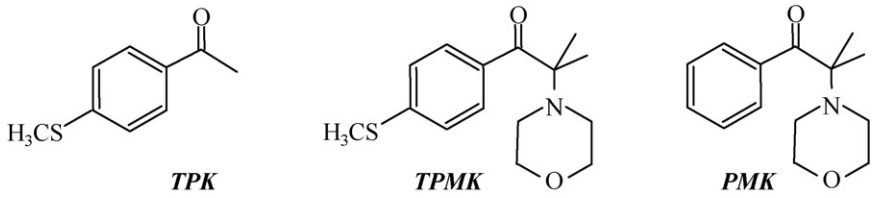

Scheme 1. Formula and abbreviations.

Scheme 2. Reaction mechanism. ISC stands for the intersystem crossing process.

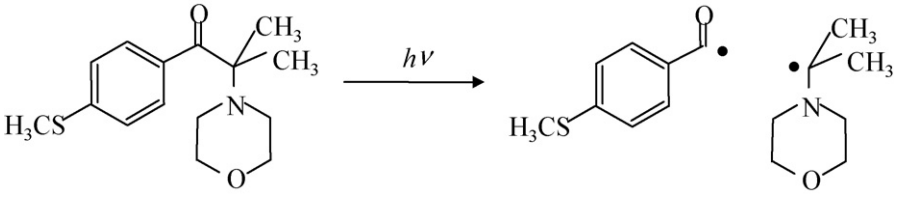

Scheme 3. Cleavage reaction upon light excitation.

picosecond laser spectroscopy and a theoretical description of the processes involved through molecular modeling.

2. Experimental

2.1. Materials

TPMK corresponds to Irgacure 907 from Ciba, Basel. PMK was received as a gift from Dr. Dietliker from Ciba, Basel. TPK (from Aldrich Chemicals) was used without further purification.

2.2. Techniques

The nanosecond laser flash photolysis set-up [10a] is based on a pulsed solid-state tunable laser and a classical transient absorption analysis system (time resolution ∼10 ns). Intersystem crossing quantum yields ϕ_{ISC} were calculated by comparing the amount of the 1-methylnaphthalene MeN triplet state formed in the BP (benzophenone)/MeN and PI/MeN interactions and considering that the ϕ_{ISC} of BP is equal to 1.

The picosecond set-up is based on the classical pump-probe arrangement [16]. The experiment consists in generating a transient species upon a short laser pulse exposure (pump pulse) and to pass a white light pulse (probe pulse) through the excited sample so that an absorption spectrum can be recorded. The fundamental (1064 nm) and the third harmonic (355 nm) emissions of a passively–actively mode locked Nd:YAG laser were, respectively, used to generate the white light continuum probe and to excite the sample (the solution is flowed through two cells, having a 2 mm optical path length). The transmitted white light is focused by appropriate lenses and injected into fiber optics directly connected to the dispersive element of a double diode arrays multichannel analyzer which will allow to get the transient optical density as a function of wavelength. A delay of up to 6 ns could be achieved between the pump and probe pulses using a computer controlled micrometer translation stage. The response function of the apparatus is ∼10 ps.

Phosphorescence spectra of the compounds were recorded on a luminescence spectrometer (Fluoromax-2, Horiba Jobin Yvon) in a glassy matrix of either 2-methyl tetrahydrofuran or isopentane (Aldrich) at 77 K. Triplet energy levels were determined from the onset of the phosphorescence spectra. A FluoroMax-4 spectrofluorometer was used for the time gated phosphorescence measurements performed in the same matrices (2-methyl tetrahydrofuran or isopentane) at 77 K. The samples are placed in a 5-mm diameter quartz tube inside a Dewar filled with liquid nitrogen. Phosphorescence anisotropy measurements were carried out using two Glan–Thompson polarizers placed in the excitation and emission beams. The anisotropy r is determined as:

$$r = \frac{I_{VV} - gI_{VH}}{I_{VV} + 2gI_{VH}} \text{ with } g = \frac{I_{HV}}{I_{HH}}$$

where I is the fluorescence intensity; the subscripts denote the orientation (horizontal H or vertical V) of the excitation and emission polarizers, respectively; g is an instrumental correction factor.

Structural and energetic factors were determined by quantum mechanical calculations using density functional theory (DFT). The hybrid functional B3LYP was used for all calculations using the 6-31G* basis set for the geometries optimization and 6-311++G** for the time-dependent calculations. All the calculations were carried out using the Gaussian 98 or Gaussian 03 suite of programs [17].

Table 1
Experimental absorption wavelengths (λ_{abs}) and extinction coefficients (ε) in acetonitrile

Compound	λ_{abs} (nm)	ε ($M^{-1}\,cm^{-1}$)	Attribution	λ_{calc} (nm)	f	Attribution
TPK				332	0.0001	nπ*
	300	22,000	ππ*	304	0.39	ππ*
PMK				383	0.0025	nπ*
	∼340	∼100–200	nπ*	339	0.0024	nπ*
	276	3700	ππ*			
TMPK				418	0.001	nπ*
	302	21,500	ππ*	311	0.20	ππ*
				304	0.25	ππ*

Calculated absorption wavelengths (λ_{calc}) and oscillator strengths (f) in gas phase at the B3LYP/6-311++G** level.

3. Results and discussion

3.1. Singlet state properties

Ground state absorption spectra are reported in Fig. 1. The UV spectra of TPK and TPMK are very similar and exhibit intense and broad absorption bands centered at 300 nm and 302 nm, respectively (Table 1), with high extinction coefficients (ε = 22,000 and 21,500 $M^{-1}\,cm^{-1}$, respectively). No significant solvent effect was observed in these cases, rendering the attribution quite difficult from the experimental UV spectra. In the case of PMK, an important absorption band is centered at 276 nm (ε = 3700 $M^{-1}\,cm^{-1}$) with a tail around 340 nm (ε = 100–200 $M^{-1}\,cm^{-1}$) decreasing slowly up to 380 nm. On the basis of the extinction coefficients, the former absorption band is attributed to a ππ* transition and the latter tail to a nπ* one. The lowest energy transition of PMK was found to be blue-shifted in polar solvents, confirming the band attribution.

More details on the absorption properties (Table 1) can be obtained from time-dependent density functional theory (TDDFT) calculations at the B3LYP/6-311++G** level. For TPK, the S_0–S_1 transition is predicted to exhibit a nπ* nature with a very low oscillator strength (f = 0.0001). It corresponds mainly to a $HOMO_{-1}$–LUMO transition centered at 332 nm. A strong S_0–S_2 absorption band corresponding to a pure ππ* HOMO–LUMO transition with a high oscillator strength (f = 0.39) is predicted at 304 nm. This result perfectly matches the observed absorption band. The typically ππ* S_0–S_3 and S_0–S_4 absorption bands are predicted to be centered at 274 and 255 nm, respectively, but with lower oscillator strengths (f = 0.0038 and 0.0001, respectively). The involved orbitals are shown in Fig. 2.

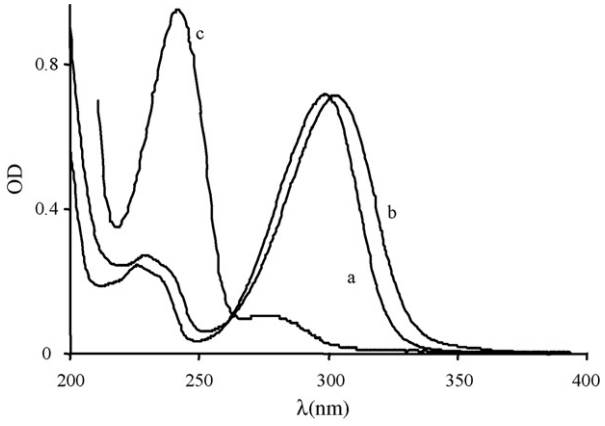

Fig. 1. Absorption spectra of (a) TPK, (b) TMPK and (c) PMK in acetonitrile.

The situation is by far more complicated for PMK. In that case, a S_0–S_1 absorption band centered at 383 nm is predicted to be a pure HOMO–LUMO transition with a moderate oscillator strength (f = 0.0025). The LUMO orbital is typically a π* MO delocalized on the whole phenyl ring. By contrast, the HOMO (Fig. 2) is a n MO mainly centered on the nitrogen atom of the morpholino moiety; a significant contribution of the morpholino C–H sigma bonds occurs through hyperconjugation. The symmetry of the n orbital on the nitrogen atom being similar to that of the LUMO π^*, this explains the relatively higher oscillator strength (usually nπ* transitions have f < 0.001). Moreover, a significant charge transfer is expected for this transition from the morpholino part to the phenyl group. The S_0–S_2 transition, predicted at 339 nm with a similar oscillator strength (f = 0.0024), is mainly $HOMO_{-1}$–LUMO nπ* involving the oxygen of the carbonyl group. The S_0–S_3 and S_0–S_4 absorption bands are also nπ* transitions, the former involving the morpholino nitrogen (281 nm, f < 0.0001) and the latter the oxygen of the carbonyl group (270 nm, f = 0.0009). The experimental absorption band with the high extinction coefficient at 276 nm corresponds to a higher electronic transition not calculated in the frame of this paper.

For TMPK, the S_0–S_1 transition is predicted at 418 nm and has a low oscillator strength (f = 0.001). This HOMO–LUMO transition is nπ*, the LUMO being very similar to that of TPK and the HOMO corresponding to that of PMK (Fig. 2). The S_0–S_2 transition is predicted at 311 nm with a high oscillator strength (f = 0.20). It corresponds to a mixed nπ*–ππ* transition. Similarly, the S_0–S_3 transition, located at 304 nm, has also a mixed nπ*–ππ* character involving the same orbitals with slightly different contributions and therefore also exhibits a high oscillator strength (f = 0.25). The S_0–S_4 transition is a $HOMO–LUMO_{+1}$ nπ* expected at 293 nm with a low oscillator strength (f = 0.0019).

As can be seen, the predicted absorption bands are in line with the experimental results. It appears (Scheme 4) that the most intense band corresponds to a S_0–S_2 transition for TPK.

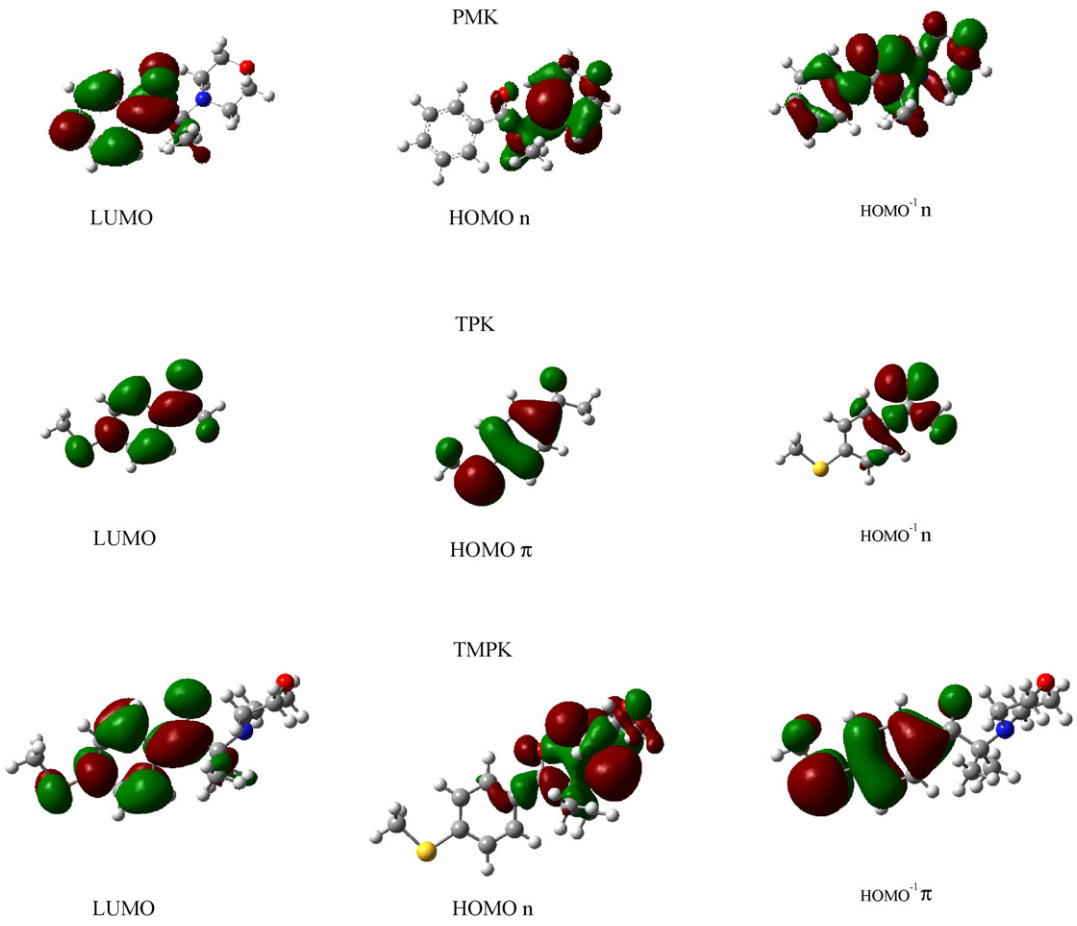

Fig. 2. Molecular orbitals involved in the S_0–S_1 and S_0–S_2 absorption of PMK, TPK and TPMK.

For TPMK, the band is a combination of the S_0–S_2 and S_0–S_3 transitions. Keeping in mind that these transitions are broadened in solution, both these singlet states are excited when using a laser excitation at 355 nm. In the case of PMK, the absorption tail corresponds to a $n\pi^*$ S_0–S_2 transition. For all the molecules, the S_0–S_1 transition probability is low. Therefore, the first excited singlet state S_1 is hardly produced by direct excitation but rather formed through internal conversion from the S_2 or S_3 excited state.

3.2. Triplet state properties

The three studied compounds exhibit a detectable phosphorescence emission in 2-methyl tetrahydrofuran at 77K (Fig. 3). TDDFT calculations at the B3LYP/6-311++G** level are used to evaluate the S_0–T_n absorption transitions, thereby giving some valuable information concerning the nature of the different triplet states. All the calculations allow to build the energy level diagram of the triplet states of the three molecules as shown in

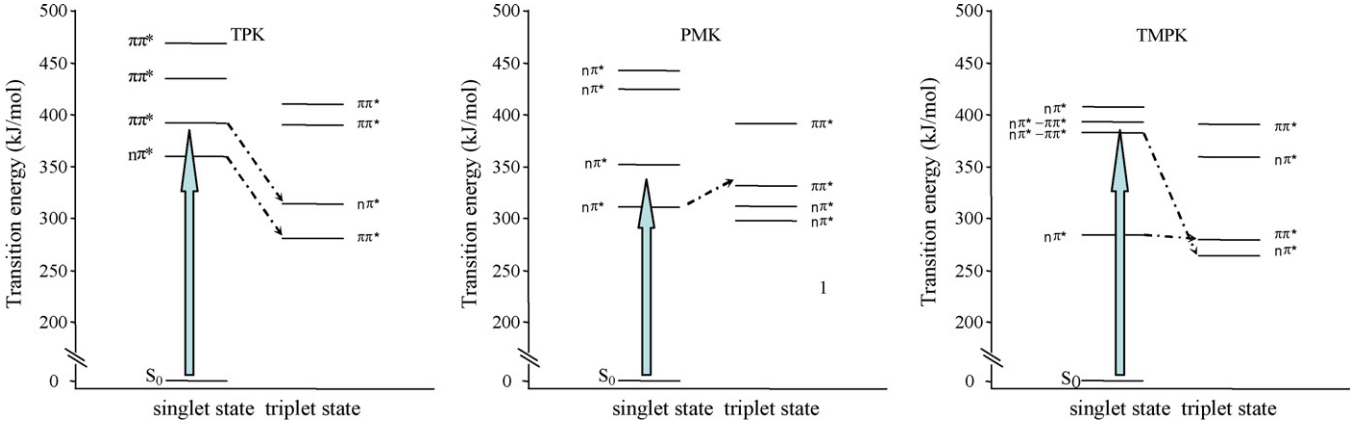

Scheme 4. Calculated singlet and triplet energy levels. The ground state absorptions at 355 nm are indicated by arrows, the allowed intersystem crossing pathways by doted arrows.

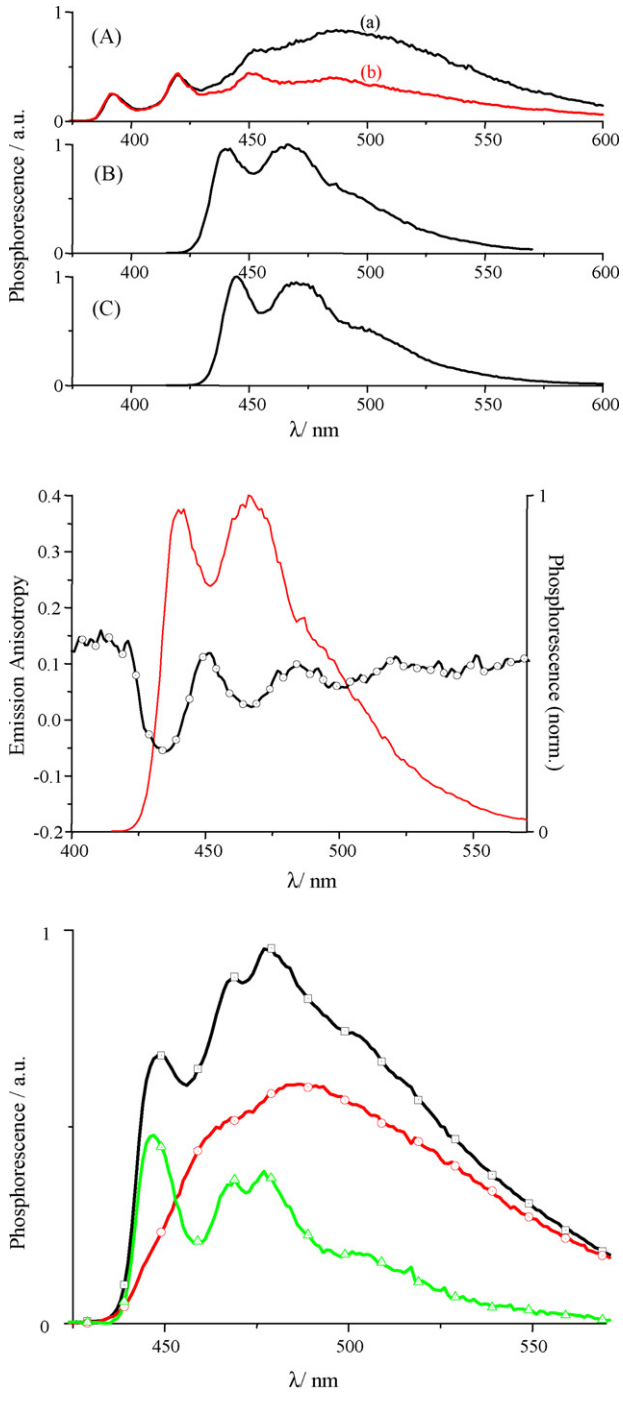

Fig. 3. Top: normalized phosphorescence spectra: (A) PMK: (a) delay: 1 ms, (b) delay: 10 ms; (B) TPK; (C) TPMK. λ_{exc} = 330 nm, solvent: 2-methyltetrahydrofuran. Middle: superimposition of the normalized phosphorescence spectrum of TPK (full line) and its corresponding emission anisotropy (open circles). λ_{exc} = 330 nm, solvent: 2-methyltetrahydrofuran. Bottom: phosphorescence spectra of TPK in glassy matrix of isopentane at two excitation wavelengths: λ_{exc} = 320 nm (open squares), λ_{exc} = 330 nm (open circles). Spectrum obtained (open triangles) by substracting these two spectra.

Scheme 4 where the allowed intersystem crossing pathways are also indicated.

PMK is weakly phosphorescent; the spectrum exhibits a broad and structureless emission band (in the 425–600 nm region, with a maximum located around 500 nm and an onset about 280 kJ/mol) and a structured emission band (in the 375–475 region, with an onset locating the emitting state around 305 kJ/mol). The existence of two emitting species is evidenced as the relative intensity contribution of each band is dependent of the phosphorescence time delay. Moreover, the phosphorescence lifetimes τ_{pho} of the blue and the red emitting species are 2.12 ms and 560 μs, respectively, which suggests a nπ* character for these two triplet states [13f]. The luminescence of the second triplet state is comparable to the emission of the T_1 state of acetophenone which also displays a typical "five-fingered" pattern and has an emission lifetime of 5.9 ms in glassy matrix of 2-methyl tetrahydrofuran. Therefore, the blue emitting species of PMK can be confidently attributed to a triplet state whose excitation is mainly localized in the acetophenone moiety. The calculations predict that the S_0–T_1 electronic excitation is nπ* with an energy of 298 kJ/mol, in very good agreement with the phosphorescence results (difference ∼6%). The fact that the transition does not significantly involve the carbonyl group explains the lack of structure for the corresponding emission band. The S_0–T_2 (312 kJ/mol, difference ∼2%) is also nπ* (mainly HOMO–LUMO) with a significant contribution of charge transfer. Both the S_0–T_3 and S_0–T_4 transitions are predicted to be ππ* (332 and 391 kJ/mol, respectively).

TPK has a phosphorescence intensity higher than that of PMK; the spectrum exhibits a structured band with an onset that, respectively, places the triplet state at 276 kJ/mol (excitation at 325 nm). The spectrum, however, is invariant upon the phosphorescence time delay. The τ_{pho} is 89.0 ms for TPK suggesting a nπ* nature for the observed triplet state. The phosphorescence anisotropy of TPK strongly fluctuates in the 420–490 nm region with a significant drop at 436 nm (with a value of −0.076) and a plateau above 500 nm (with a value of 0.058). Such anisotropy variations clearly indicate an emission from two triplet states; the fact that only one lifetime can be measured indicates a fast equilibrium between the two states which should be very close. In addition, the excitation spectrum recorded at 516 nm broadens to the red by ∼4 nm compared to that recorded at the 434 nm emission wavelength in isopentane. This latter experiment gives a chance to specifically record the long wavelength emission spectrum by exciting at 330 nm. Substracting this component to the whole phosphorescence spectrum recorded by exciting at 320 nm allows to visualize these two emitting triplet states. It turns out that the lowest triplet state exhibits a broad and structureless band with a maximum at 485 nm. The calculation of the onset is not straightforward. However, a value of about 265–275 kJ/mol can be estimated. The upper triplet state exhibits a vibrationnal structure indicating a nπ* T_2 state with a maximum at 447 nm and an onset leading to an energy of 279 kJ/mol. Calculations on TPK shows that the nature of the S_0–T_1 electronic transition is typically ππ* and the corresponding energy is 281 kJ/mol which also matches quite well the experimental result. The S_0–T_2 transition is typically nπ* with an energy about 314 kJ/mol. Both upper transitions (S_0–T_3 and S_0–T_4) are ππ* (406 and 412 kJ/mol, respectively). The discrepancy for the spectroscopic character of the lowest lying triplet state is attributed to the relaxation which renders the ^{3}nπ* level lower than the ππ* triplet

state (this is confirmed by the calculations of the MOs which show an inversion of the n and π orbitals in the relaxed triplet state).

The same behavior is observed for TPMK which exhibits a structured phosphorescence spectrum with an onset that places the triplet state at 273 kJ/mol (excitation at 325 nm). The existence of the two emitting triplet states is also highlighted by emission anisotropy measurements. In this case, the anisotropy displays a minimum at 437 nm (−0.072) and gets invariant above 490 nm with a value of 0.058. As in TPK, only one value is found for τ_{pho} (97.4 ms, supporting a $^3n\pi^*$ state) which suggests the presence of two close lying triplet states. The computations show that the S_0–T_1 is mainly nπ* with an energy of 265 kJ/mol, quite close to the phosphorescence results (difference ∼4%) and in agreement with the assignment of Ref. [18]. The S_0–T_2 transition (280 kJ/mol) is ππ*, S_0–T_3 is nπ* (359 kJ/mol) and S_0–T_4 is ππ* (391 kJ/mol).

3.3. Laser flash photolysis (LFP)

3.3.1. Nanosecond LFP

The transient absorption spectra of TPK and TPMK were recorded in benzene in the nanosecond time scale. Both transient absorption spectra exhibit a similar broad band centered around 450 nm (Fig. 4). A small residual for TPMK is observed in the 360–420 nm range; it might be attributed to the methylthiobenzoyl radical. The lifetimes of the transient species are 2.3 μs and 10 ± 2 ns (after deconvolution) for TPK and TPMK, respectively. On the basis of energy transfer experiments using camphorquinone for TPK and 1-methylnaphthalene for TPMK, these transient species were attributed to the triplet states of the molecules.

The PMK transient species exhibits low molar extinction coefficients and second order kinetics attributed to the recombination of the radicals formed after photodissociation. An energy transfer experiment with 1-methylnaphthalene MeN was carried out: following the growth of the optical density of the MeN triplet state confirms an estimate of the PMK triplet state lifetime lower than 1 ns.

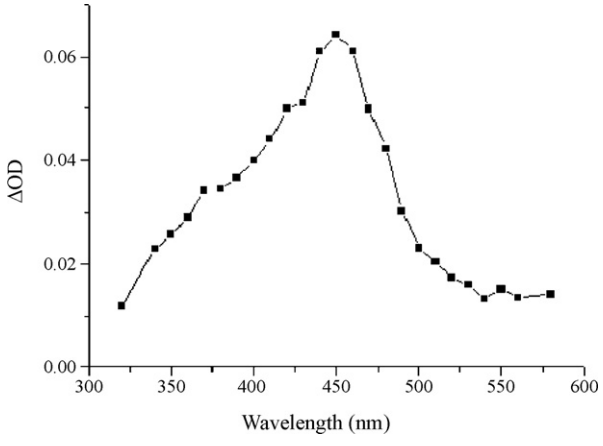

Fig. 4. Transient absorption spectrum for TPK in benzene recorded 300 ns after excitation at 355 nm. OD_{355nm} = 0.2.

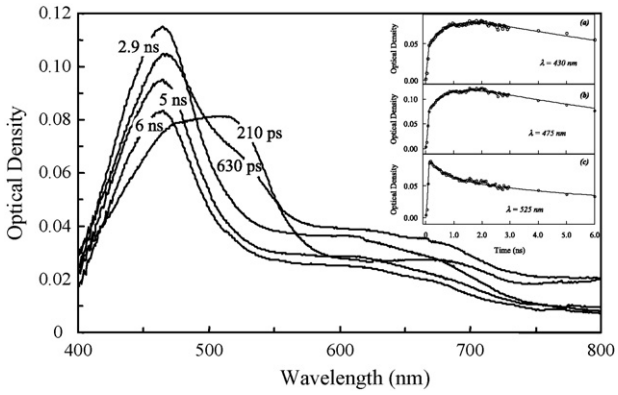

Fig. 5. Transient absorption spectra of TPMK in benzene monitored at several delay times after excitation. Inset: experimental (◯) and calculated (—) transient kinetics monitored at (a) 430 nm, (b) 475 nm and (c) 525 nm. The following set of values has been used: τb = 700 ps, and τc = 10 ns. See text.

3.3.2. Picosecond LFP

3.3.2.1. Transient spectra and kinetics of TMPK. Fig. 5 displays the transient absorption spectra of TPMK in benzene gathered at different time delays between the pump and the probe pulses. After 210 ps, the spectrum is characterized by an absorption (with a maximum around 500 nm) that spreads over a wide spectral range (400–800 nm). As the delay increases (up to 3 ns), the absorption at 525 nm decreases and a rather sharp band is clearly detected at 460 nm. For longer time delays (from 3 to 6 ns), the spectrum remains unchanged. The band at 460 nm is ascribed to the absorption of the TPMK excited triplet state (as expected from Fig. 4); a possible contribution of the methylthiobenzoyl radical can be expected (see above) but it should be very low in the present time scale. The strong change around 525 nm, noted between time 210 and 630 ps is likely due to the presence of a singlet-singlet absorption originating from a short-lived singlet state (<1 ns). As a consequence, three types of absorption are assumed to be present. The time evolution of the transients (Fig. 5) was monitored at several wavelengths (430, 475, and 525 nm). The kinetics are rather similar at 430 and 475 nm with a fast rise, a slow rise and a slow decay of the transient absorption. At 525 nm, the absorption is only characterized by a fast rise and a slow one-component decay.

Energy transfer confirms the above assignments. The absorption spectra in the presence of naphthalene (E_T = 253 kcal mol^{-1} [19]), taken between 150 ps and 2100 ps every 150 ps, are displayed in Fig. 6: a decrease of the original absorption above 450 nm as well as the appearance of a sharp absorption band due to the naphthalene triplet state (known to absorb around 420 nm [18]) are clearly observed. The corresponding kinetic traces at the wavelengths selected before are reported in the inset of Fig. 6.

Based on Scheme 4, a four state kinetic model satisfying to the El-Sayed selection rules for the intersystem crossing was used to describe the primary processes in TPMK (Scheme 5).

In this model, the S_0 ground state absorption leads to the second excited singlet ππ*state S_2. A non-radiative relaxation process deactivates this state down to the first excited singlet nπ* state S_1. Then, the ππ* T_2 and nπ* T_1 triplet states are popu-

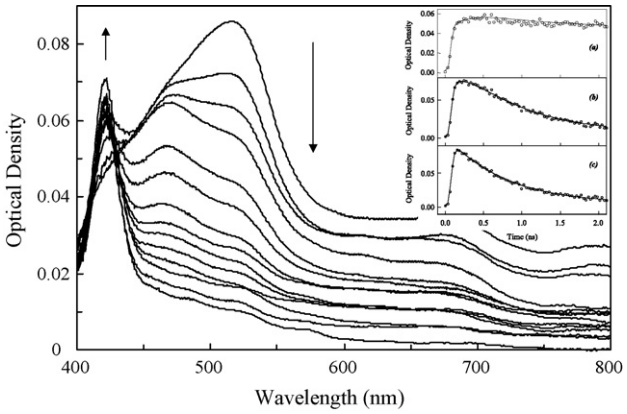

Fig. 6. Evolution of the transient absorption of TPMK/naphthalene (0.5 M) in benzene. The experiment started at 150 ps and ended at 2100 ps after the pump pulse. The spectra are taken every 150 ps. Inset: transient kinetics followed at (a) 430 nm, (b) 475 nm and (c) 525 nm. The following set of values has been used: $\tau b = 700$ ps, and $\tau c = 300$ ps. See text.

lated through intersystem crossing from S_1 and S_2, respectively. Symbols k_{ic1} and k_{ic2} are the internal conversion rate constants, k_{isc1} and k_{isc2} the intersystem crossing rate constants, k_{d1} and k_{d2} the deactivation rate constants of the $^1\pi\pi^*$ and $^1n\pi^*$ singlet states, k' the rate constant of the T_1 relaxation, k_{diss} the rate constant of the α-cleavage from the $^3n\pi^*$ excited triplet state. The lifetimes of the S_1 (τb), S_2 (τa), T_1 (τc) and T_2 (τd) states are expressed by the following expression where τa and τd should be lower than 10 ps:

$$\tau a = \frac{1}{k_{ic1} + k_{isc1} + k_{d1}}; \tau b = \frac{1}{k_{d2} + k_{isc2}}; \tau c = \frac{1}{k_{diss} + k'}; \tau d = \frac{1}{k_{ic2}}$$

The overall transient optical density is calculated as the sum of the terms corresponding to the absorptions of S_1, T_1, the radicals (to a lesser extent) and the naphthalene triplet state when present. The transient kinetics displayed in the insets of Figs. 5 and 6 are quite well fitted according to this model. It appears that the T_2 state is populated within 700 ps and leads to the T_1 state through a very fast internal conversion. The T_1 state is also

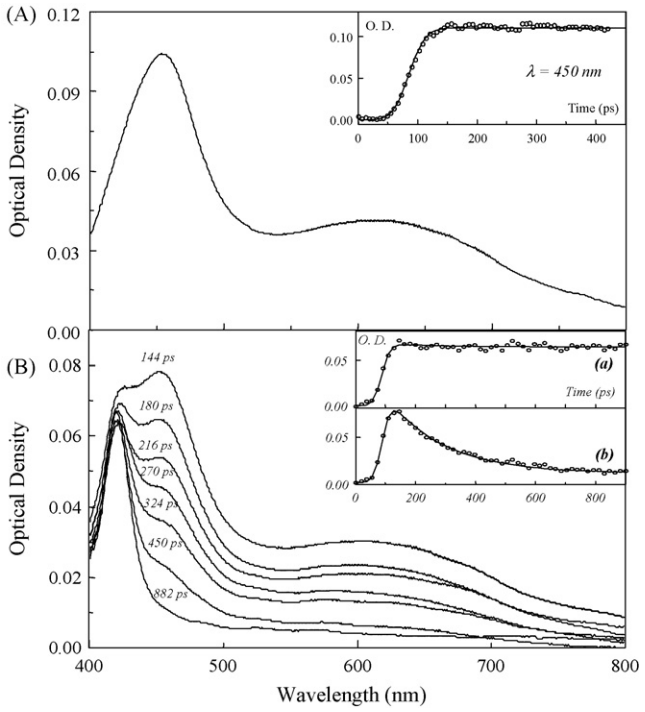

Fig. 7. (A) Transient absorption spectrum for TPK in benzene recorded with a time delay of 1 ns after the excitation at 355 nm. Inset: experimental (◯) and calculated (—) kinetics at 450 nm. (B) Evolution of the overall absorption of TPK/naphthalene (0.5 M) in benzene at different time delays after the excitation pulse. Inset: experimental (◯) and calculated (—) transient decay monitored at (a) 420 nm and (b) 450 nm.

directly populated from S_2 within the time response of the apparatus (10 ps). The lowest spectroscopic T_1 state has a lifetime of 10 ns which yields a value of $10^8\ s^{-1}$ as the lower limit for the cleavage rate constant. When naphthalene 0.5 M is added, the T_1 lifetime drops to 300 ps and the calculated quenching rate constant ($6.4 \times 10^9\ M^{-1}\ s^{-1}$) is close to another reported value for naphtalene [3].

3.3.2.2. Transient spectra and kinetics of TPK. The observed transient spectrum for TPK in benzene reported in Fig. 7A spreads from 400 to 800 nm and exhibits two bands: an intense one at 450 nm and a broader one (with a lower intensity) centered

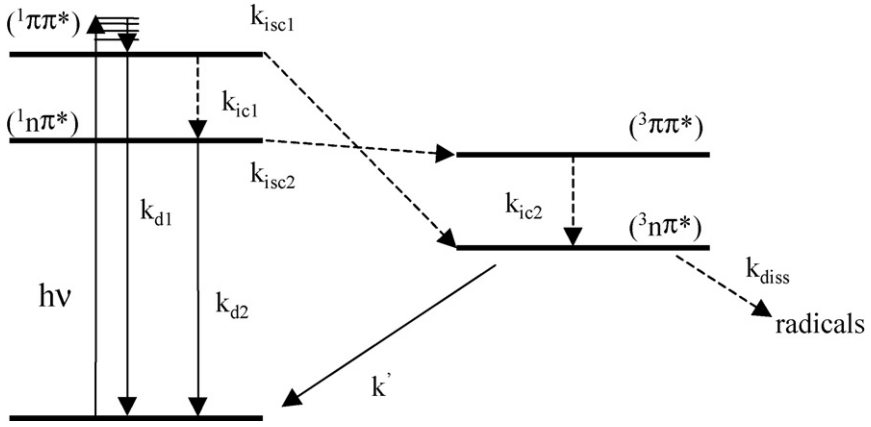

Scheme 5. Kinetic model used for TPMK.

around 610 nm. The inset shows the shape of the typical transient kinetics observed whatever the wavelength and consisting in a fast rise followed by a plateau. As depicted in Fig. 7B, this transient is quenched by naphthalene as revealed by a fast disappearance of the original absorption (e.g. at 450 nm) together with the appearance of the naphthalene triplet state at 420 nm.

The laser excitation forms the S_2 state. According to the above discussion, the model involves four states: S_2 ($\pi\pi^*$), S_1 ($n\pi^*$), T_2 ($\pi\pi^*$) and T_1 ($n\pi^*$) similar to those of TPMK (Scheme 5) but the available experimental data rule out the possibility for the kinetic treatment to settle once and for all this scheme. A fit of the decay trace is reported in the inset of Fig. 7 where the decay at 450 nm yields a bimolecular TPK/naphthalene quenching rate constant (5×10^9 M^{-1} s^{-1}) almost similar to the value used in [3] for naphtalene. The ISC rate constant is estimated to be higher than 10^{11} s^{-1} (within the time response of the apparatus). The highly efficient naphthalene quenching is in line with the $^3n\pi^*$ character of T_1.

3.3.2.3. Transient spectra and kinetics of PMK. The picosecond laser excitation of PMK in benzene leads to a short-lived transient absorption around 485 nm (Fig. 8) which is not quenched by naphthalene. This absorption is therefore ascribed to that of the first excited singlet state S_1. The energy transfer experiment leads to a slight modification of the absorption around 420 nm supporting the presence of a triplet state (as already demonstrated above by LFP quenching experiments). The overall process can be depicted by the sequence shown in

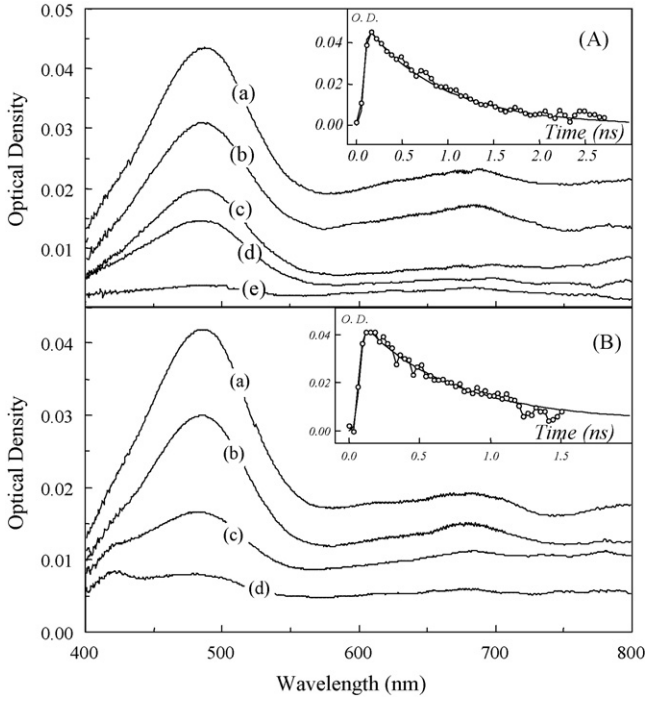

Fig. 8. Evolution of the overall absorption of PMK in benzene at different pump-probe delays after the excitation pulse. A: in the absence of naphthalene; (a) 220 ps, (b) 540 ps, (c) 870 ps, (d) 1190 ps, (e) 2700 ps. B: in the presence of naphthalene 0.5 M; (a) 180 ps, (b) 420 ps, (c) 960 ps, (d) 1500 ps. Inset: experimental (◯) and calculated (—) transient absorption decay monitored at 475 nm.

Table 2
Singlet ($^1n\pi^*$) and triplet ($^3n\pi^*$) state lifetimes of TPMK in various solvents (classified according to their polarity)

Solvents	S_1 lifetime (ps)	T_1 lifetime (ns)
Benzene	700	10
Tetrahydrofuran	500	6.5
Ethylacetate	700	4.2
1,2-Dichloroethane	750	4.8
Dimethylformamide	370	5.2
Acetonitrile	500	6.3
2-Propanol	100	2.7
Ethanol	40	1.0

Scheme 4: very fast population of S_1 from S_2, then of T_3 from S_1 (and T_1 from T_3); the intersystem crossing S_2–T_3 might occur if it can compete with the S_2–S_1 internal conversion. In the absence of a significant detectable effect of the naphthalene quenching on the kinetic traces (due to the strong absorption of the S_1 state), no model can be obviously tested for PMK. The S_1 lifetime is 700 ps: the intersystem crossing should occur within 700 ps.

3.3.2.4. Transient spectra and kinetics of TMPK in different solvents. The behavior of TPMK has been also considered in several solvents. The same trends are observed. The S_1 and T_1 lifetimes, shown in Table 2, tend to decrease as the polarity of the medium increases. Possible explanations for this behavior can be the following. First, in polar hydroxylic solvents, the $^1\pi\pi^*$ states are stabilized whereas the $^1n\pi^*$ states are destabilized because of the solute–solvent interactions (polarity/polarizability and hydrogen bonding); thus the energy gap between S_1 ($^1n\pi^*$) and S_2 ($^1\pi\pi^*$) decreases, enforcing the $\pi\pi^*$ character of the S_1 state and shortening its lifetime. Second, the polarity of the solvent stabilizes the polar transition state exhibiting a partial positive charge at the α carbon (expected in cleavable ketones): this would lower the barrier for the α-cleavage, increase the rate constant and, as a consequence, decrease the $^3n\pi$ state lifetime. Third, the occurrence of a strong intermolecular hydrogen bond could increase the reactivity by locking the ketone in a favorable conformation as observed in benzoin [14c] and hydroxyl acetophenone derivatives [14b].

4. Conclusion

In this paper, the role of the para thioether substitution on a benzoyl group as well as the hyperconjugation with a substituent (morpholino one) introduced at the α carbon position is outlined. The derived kinetic models for the excited state processes perfectly fit the experimental results. From a general point of view, our work clearly shows that a combined approach based on steady-state experiments, time-resolved laser spectroscopy and molecular modeling calculations allows to characterize the involved molecular orbitals, to explain the observed transitions and to propose a diagram of singlet and triplet energy levels. This kind of work opens up a new insight into the ground state absorption properties and the excited state reactivity of photoinitiators.

References

[1] (a) J.P. Fouassier, Photoinitiation, Photopolymerization, Photocuring, Hanser, Münich, 1995;
(b) J.P. Fouassier (Ed.), Photochemistry and UV Curing: New Trends, Research Signpost, 2006;
(c) K. Dietliker, A Compilation of Photoinitiators Commercially Available for UV Today, Sita Technology Ltd., London, 2002;
(d) Photoinitiated Polymerization, in: K.D. Belfied, J.V. Crivello (Eds.), ACS Symposium series 847, Washington DC, 2003.

[2] L. Angiolini, D. Caretti, E. Salatelli, Macromol. Chem. Phys. 201 (18) (2000) 2646.

[3] R. Liskra, D. Herzog, J. Polym. Sci. Part A: Polym. Chem. 42 (3) (2004) 752–764.

[4] K. Sirovatka Padon, A.B. Scranton, J. Polym. Sci. Part A: Polym. Chem. 38 (2000) 3336.

[5] F. Catalina, C. Peinado, M. Blanco, T. Corrales, N.S. Allen, Polymer 42 (5) (2000) 1825–1832.

[6] J. Kabatc, B. Jedrzejewska, J. Paczkowski, J. Polym. Sci. Part A: Polym. Chem. 38 (13) (2000) 2365–2374.

[7] I. Gatlik, P. Rzadek, G. Gescheidt, G. Rist, B. Hellrung, J. Wirz, K. Dietliker, G. Hug, M. Kunz, J.P. Wolf, J. Am. Chem. Soc. 121 (36) (1999) 8332–8336.

[8] J. Alvarez, M.V. Encinas, E.A. Lissi, Macromol. Chem. Phys. 200 (10) (1999) 2411.

[9] R.S. Davidson, H.J. Hageman, S.P. Lewis, J. Photochem. Photobiol. A 118 (3) (1998) 183.

[10] (a) J.P. Fouassier, X. Allonas, J. Lalevée, M. Visconti, J. Polym. Sci. Part A: Polym. Chem. 38 (2000) 4531–4541;
(b) J.P. Malval, C. Dietlin, X. Allonas, J.P. Fouassier, J. Photochem. Photobiol., A : Chem. 192 (2007) 66–73;
(c) J. Lalevée, X. Allonas, S. Jradi, J.P. Fouassier, Macromolecules 39 (2006) 1872–1879;
(d) J.P. Fouassier, D.J. Lougnot, J.C. Scaiano, Chem. Phys. Lett. 160 (1989) 335–340.

[11] (a) S. Jockusch, M.S. Landis, B. Freiermuth, N.J. Turro, Macromolecules 34 (6) (2001) 1619–1626;
(b) S. Jockusch, I.V. Koptyug, P.F. McGarry, G.W. Sluggett, N.J. Turro, D.M. Watkins, J. Am. Chem. Soc. 119 (47) (1997) 11495–11501.

[12] F. Bosca, G. Cosa, M.A. Miranda, J.C. Scaiano, Photochem. Photobiol. Sci. 1 (2002) 704–708.

[13] (a) F.D. Lewis, R.T. Lauterbach, H.G. Heine, W. Hartmann, H. Rudolph, J. Am. Chem. Soc. 97 (6) (1975) 1519–1525;
(b) L. Salem, J. Am. Chem. Soc. 96 (1974) 3486;
(c) W.G. Dauben, L. Salem, N.J. Turro, Acc. Chem. Res. 8 (1975) 41;
(d) L.G. Arnaut, S.J. Formosinho, J. Photochem. 31 (1985) 315–332;
(e) N.J. Turro, Modern Molecular Photochemistry, University Science Books, Sausalito, CA, 1991.

[14] (a) M. Spichty, N.J. Turro, G. Rist, J.L. Birbaum, K. Dietliker, J.P. Wolf, G. Gescheidt, J. Photochem. 142 (2001) 209;
(b) X. Allonas, F. Morlet Savary, J. Lalevée, J.P. Fouassier, Photochem. Photobiol. 82 (2006) 88;
(c) M. Lipson, N.J. Turro, J. Photochem. 99 (1999) 93–96;
(d) J. Lalevée, X. Allonas, C. Grotzinger, J.P. Fouassier, M. Visconti, G. Li Bassi, in: J.P. Fouassier (Ed.), Photochemistry and UV Curing: New Trends, Research Signpost, 2006, pp. 79–90.

[15] D. Ruhlman, J.P. Fouassier, Eur. Polym. J. 28 (6) (1992) 591.

[16] F. Morlet Savary, C. Ley, P. Jacques, J.P. Fouassier, J. Phys. Chem. 105 (2001) 11026–11033.

[17] M.J. Frisch, G.W. Trucks, H.B. Schlegel, G.E. Scuseria, M.A. Robb, J.R. Cheeseman, V.G. Zakrzewski, J.A. Montgomery Jr., R.E. Stratmann, J.C. Burant, S. Dapprich, J.M. Millam, A.D. Daniels, K.N. Kudin, M.C. Strain, O. Farkas, J. Tomasi, V. Barone, M. Cossi, R. Cammi, B. Mennucci, C. Pomelli, C. Adamo, S. Clifford, J. Ochterski, G.A. Petersson, P.Y. Ayala, Q. Cui, K. Morokuma, P. Salvador, J.J. Dannenberg, D.K. Malick, A.D. Rabuck, K. Raghavachari, J.B. Foresman, J. Cioslowski, J.V. Ortiz, A.G. Baboul, B.B. Stefanov, G. Liu, A. Liashenko, P. Piskorz, I. Komaromi, R. Gomperts, R.L. Martin, D.J. Fox, T. Keith, M.A. Al-Laham, C.Y. Peng, A. Nanayakkara, M. Challacombe, P.M.W. Gill, B. Johnson, W. Chen, M.W. Wong, J.L. Andres, C. Gonzalez, M. Head-Gordon, E.S. Replogle, J.A. Pople, Gaussian 98, Revision A. 11, Gaussian, Inc., Pittsburgh PA, 2001.

[18] R.H. Compton, K.T.V. Grattan, T. Morrow, J. Photochem. 14 (1980) 61–66.

[19] S.L. Murov, I. Carmichael, G.L. Hug, Handbook of Photochemistry, 2nd ed., Marcel Dekker, 1993 (Rev. and exp.).